Jour. Korean Earth Science Society, v. 34, no. 5, p. 415−427, September 2013 ISSN 1225-6692 (printed edition)
http://dx.doi.org/10.5467/JKESS.2013.34.5.415 ISSN 2287-4518 (electronic edition)

A *BVR* Photometric Survey of the Small Magellanic Cloud with a Mosaic CCD

Ki-Won Lee*

Institute of Liberal Education, Catholic University of Daegu, Gyeongbuk 712-702, Korea

Abstract: We performed a *BVR* photometric survey for the entire Small Magellanic Cloud (~26 deg^2) with a mosaic system, Wide Field Imager (WFI), covering three seasons: September and October 2001 and November 2002. Through the usual data reduction procedures, we present ~0.73 million catalogue stars brighter than 19 magnitude in *B* amongst a total of ~1.3 million and compare them with published astrometry and photometry results. We found that the average differences between our and the published data are ~0.7 arcsec in astrometry and 0.065, 0.054, and 0.163 in *B*, *V*, and *R*, respectively, in photometry. In addition, using the 2dF spectroscopic data from Evans et al. (2004), we determined the color excesses in (*B-V*) and (*V-R*) to be 0.086±0.156, and 0.065±0.112, respectively, while for the distance modulus, we obtained 18.55±1.05.

Keywords: catalogue, photometry, Small Magellanic Cloud, survey

Introduction

The Small Magellanic Cloud (SMC) is an irregular dwarf galaxy in the southern constellation of Tucana. The main body of SMC was designated NGC 292 in the New General Catalogue. Together with the Large Magellanic Cloud (LMC), the SMC makes up a satellite galaxy to the Milky Way.

Arp (1962) first noted that the SMC has a different metallicity compared to the solar neighborhood. According to Lequeux et al. (1979), the metallicity of the SMC is $Z_{SMC}=0.1Z_{\odot}$. Because of its proximity and lower metallicity, there have been many studies on SMC in both the photometric and spectroscopic realms. Azzopardi and Vigneau (1975, 1982) presented a catalogue of 524 SMC stars including both *UBV* photometric and spectroscopic data. Later, the OGLE group (Udalski et al., 1998) published a *BVI* catalogue for the central regions of the SMC bar. More recently, Zaritsky et al. (2002) presented a *UBVI* photometric survey of the central 18 deg^2 and Massey (2002) performed a *UBVR* survey for the 7.2 deg^2 of the SMC. Evans et al. (2004) used intermediate-resolution 2dF spectroscopy and classified 4054 stars in the MK system. Very recently, Bonanos et al. (2010) performed infrared photometry of 5324 massive stars in the SMC. Thus, SMC is now one of the most well-studied galaxies, but there are ongoing debates on the structure of the SMC, its evolutionary status, the effect of lower metallicity on the stellar evolution, and so on. General reviews of SMC can be found in van den Bergh (2000) and Westerlund (1997).

However, there have been no attempts to photometrically survey the entire SMC area. In order to accomplish this goal, we performed a *BVR* photometric survey during three seasons. We summarize the observations and describe the data reductions in section 2. In section 3, we present our SMC catalogue and compare it with other published ones in terms of astrometry and photometry. Finally, the summary is given in section 4.

*Corresponding author: leekw@cu.ac.kr
Tel: +82-53-850-2573
Fax: +82-53-850-3800

Observations and Data Reductions

Observations

Observations were made with the 40-inch telescope at the Siding Spring Observatory (SSO) in Australia, using the Wide Field Imager (WFI) during 5-11 September and 26-31 October 2001, and 9-17 November 2002. The WFI is a focal-plane CCD system with a size of 123 by 123 mm and having 8192 by 8192 pixels, comprising a 4×2 array of thinned, back-illuminated, 2048×4096 pixel CCDs. Each CCD covers 13'×26' (arcmin) making a total field of 52'×52'. The pixels have a size of 15 μm giving 0.375 arcsec/pixel (at f/8). The most useful aspect is that the controller reads out the entire array in only 55 seconds. However, in order to increase the charge transfer efficiency, the WFI has a relatively warm operating temperature of ~183K for the focal-plane. The penalty for this is an increased dark current, which is not flat. In Fig. 1, we present the layout of the WFI system.

To obtain multicolor photometry for hot stars in the whole SMC area, we divided it into 35 fields (see Fig. 2) and used *B*, *V*, and *R* filters with two sets of exposure times, i.e., 60 and 600 seconds; the shorter exposures permit photometry of stars that are saturated in longer observations. In order to get an accurate *B* magnitude, we obtained two 600 s object frames in each field. In addition, to compensate for the gap between each CCD (~20-30 arcsec), we obtained one or two dithered frames. The 'b' (or 'c') suffix at the end of the grid number represents the first (or second) dithered frame for the grid 'a'. In the 2002 observations, we also obtained repeat exposures of some previously observed fields for the purpose of checking systematic differences between the two epochs and investigating further frame-matching in the overall mosaic image. The general features of each observation are briefly summarized in the following subsections.

September 2001: The most notable feature of these data is that there was a readout problem in the #01a, #01b, #02a, and #02b grid data. Thus, parts of each CCD image are shifted into the next CCD, especially in the #1-#4 CCDs. To correct those frames, we found the boundary of each of the shifted parts by inspection and moved them into the correct CCD chips. The average full-width at half-maximum (FWHM) in this run is 8.1 pixels, corresponding to 3.0 arcsec.

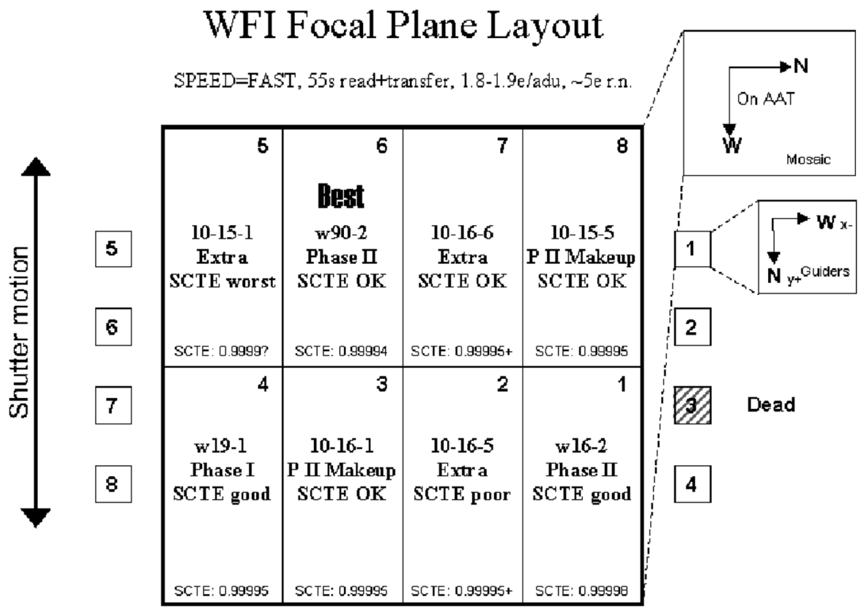

Fig. 1. WFI focal plane layout showing assigned number, quality, and manufacture for each CCD chip.

October 2001: Some of the October 2001 data have missing information, such as the exposure time and filter name, in the data header file; therefore, we inserted them based on log files. In order to compensate for the problems in the fields mentioned for the September 2001 data, we re-observed for those areas in the middle of the October observations (October 29). In this run, the average FWHM is 3.0 arcsec.

November 2002: The purpose of these observations was to finish the remaining fields of the SMC. However, we found two remarkable changes in the CCD chips during the observations: an increase of the bias levels (over 100 ADU) in CCD chip #1, #3, and #5, and a sudden appearance of hot pixels between the 550 and 820 columns in the #6 CCD chip from November 14 onwards. To compensate for this, we constructed two master bias and dark frames and separately applied them to the other frames. The average FWHM of these observations was 4.2 arcsec, which is the largest average value amongst the runs. The worst individual observation was 5.7 arcsec on November 16, 2002.

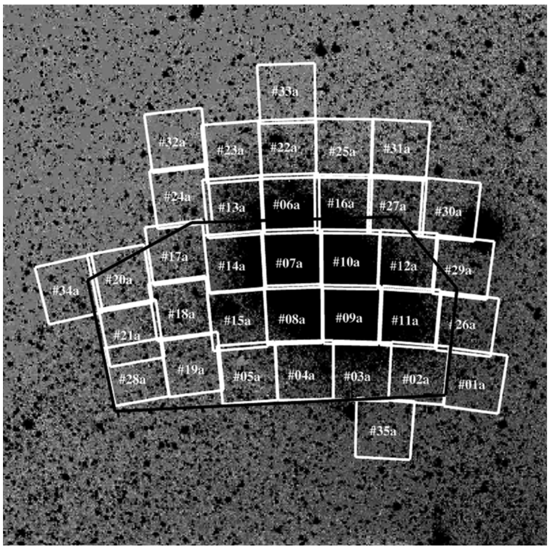

Fig. 2. Outlines of our grid field (small white boxes) and 2dF spectroscopic area from Evans et al. (2004) (large black box) are shown against this image of the SMC. Only each 'a' grid is shown for the purpose of illustration. North is to the top and east is to the left.

Data reductions

The reduction procedure for the mosaic and single CCDs is essentially identical if the former is treated independently for each chip. However, excellent reduction tools exist, such as the Image Reduction and Analysis Facility (IRAF) package, MSCRED, which allows each chip to be dealt with simultaneously. In the following, we give a concise description of some of the noteworthy steps in our data reductions and standardization.

Linearity correction: After the correction of the master bias frame (or zero frame), we applied a polynomial linearity correction to the WFI data using the equation and coefficients given in the technical notes. Unfortunately, the MSCRED package of IRAF does not support a linearity correction task for the dark frame. Hence, we split each multiextension FITS (MEF) file into individual ones, inserted coefficient values in each file header, calculated the linearity using the IMEXPR task, and then rejoin the files.

Dark correction: As mentioned above, the WFI data should be corrected by the master dark frames differently with modern astronomical CCD data. The master dark frames were created according to the exposure times of our astronomical frames (i.e., 60 s and 600 s). We found that the dark current rate levels in the 60 s astronomical images are negligible. However, we apply the correction nonetheless for completeness and consistency.

Sky flat field correction: As Valdes (2002) pointed out, mosaic system data generally need a secondary flat-fielding because of their large field of view. We obtained twilight flat frames after sunset and before sunrise whenever the weather permitted, made master flat frames from those obtained during each run, and applied them to all object frames taken from the same run. Next, we generate daily master sky flat frames, because the background sky levels vary daily, even within hours in a day and between regions, with the SFLATCOMBINE task using the twilight flat field corrected object frames obtained the same day. Again, we apply them to all the object frames to give secondary flat-fielding corrections.

World coordinate system: One of the important elements in a mosaic survey is the World Coordinate System (WCS) information in order to identify stars located in dithered and/or overlapping frames. However, the WFI data have no WCS information; therefore, we had to manually create an initial WCS file containing physical coordinates (*x* and *y*) and their corresponding celestial coordinates (RA and Dec) with the eye-identification of a couple of stars for each chip. Moreover, because of the poor pointing and inaccurate RA and Dec information, the initial WCS data file is only valid for the grid frames taken on the same day. Thus, it does not work for dithered frames even for the same grid taken on different days. After creating the initial WCS, we improved the accuracy using a software named WCStool (Mink 1996, 1997, 1999).

Standardization: In order to increase the photometric accuracy, we performed photometry for each CCD chip, neither stacked nor singled mosaic image, using the DAOPHOT package (Stetson, 1987). One of the disadvantages of mosaic CCD observation is that it is difficult to obtain a standard star frame containing a couple of standards in each chip (eight chips in WFI). Therefore, we used the Massey (2002) catalogue stars with $\sigma \leq 0.02^{m}$ in each filter as the standard stars. The formulae for our standardization transformation

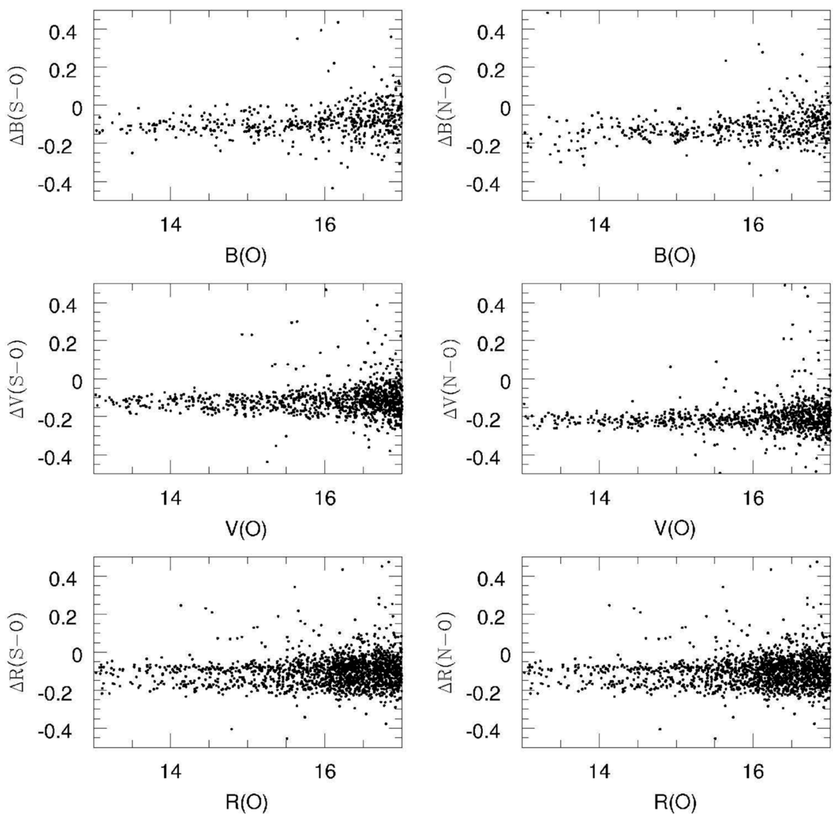

Fig. 3. The seasonal magnitude differences in *B*, *V*, and *R* from grid #02a. The *x*-axis shows the October 2001 data (O) and *y*-axis shows magnitude difference between September and October $\Delta(S-O)$ in left panel and November and October $\Delta(N-O)$ in right panel. The top, middle, and bottom in each panel represent difference in *B*, *V*, and *R* magnitudes, respectively.

equations are given by:

$$V = v + c_V + \varepsilon_V\ (B-V),$$
$$(B-V) = c_{BV} + \varepsilon_{BV}\ (b-v),$$
$$(V-R) = c_{VR} + \varepsilon_{VR}\ (v-r), \quad (1)$$

where v, b, and r are instrument magnitudes in the V, B, and R magnitudes, c's are normalization constants, and ε's are color terms (see Lee, 2005).

As a check of the seasonal difference in magnitudes, we selected 600 s exposure frames of the grid element #02a, the element for which we have observations covering the same area of the sky for the three runs with good photometry. We choose the October 2001 data as our reference because they are in the middle of the seasonal sequence and have the best FWHM amongst the element #02a data. Fig. 3 shows the difference in magnitudes in each filter for the September 2001 (S) and November 2002 (N) data with respect to the October 2001 data (O). On average, the magnitude difference with the September 2001 data is ~0.1 and that with November 2002 is ~0.2.

To take into account the different numbers of counts recorded in different frames, we calculated their weighted mean to obtain a final magnitude and its standard deviation. After identifying a star recorded in different frames, we found the median value and selected only those having a difference equal to or less than 0.1 for that value. If the magnitude of all stars used in the calibration of a weighted magnitude (of course, except for their median star) show a spread greater than 0.1 compared to their median, we flag it as '99' instead of using the star's numbers in our catalogue (refer to Table 1) and simply use the median as the magnitude.

Results

Here, we describe our SMC catalogue and the results of completeness test both in the survey area and photometry sides. The comparison with other published catalogues is also given in terms of astrometry and photometry. We present the color magnitude diagrams of $(B-V)$ versus V and $(V-R)$ versus V. In addition, using the 2dF spectroscopic data from Evans et al. (2004), we estimate the color excesses in $(B-V)$ and $(V-R)$ indices and the distance modulus.

The SMC catalogue

Table 1 shows a portion of our whole SMC catalogue in B, V, and R sorted in order of right ascension (RA). Column 1 is the sequential identifier. Columns 2 and 3 are, respectively, the RA (degrees) and declination (DEC, degrees) in the J2000 epoch. Columns 4, 7, and 10 represent the magnitude in B, V,

Table 1. A portion of the full SMC catalogue brighter than 19 magnitude in B

ID	RA[1]	DEC[2]	B	σ_B	Flag	V	σ_V	Flag	R	σ_R	Flag
0000001	3.54173708	-74.68917084	17.670	0.022	1	17.996	0.033	1	17.517	0.025	1
0000002	3.54325533	-74.51149750	18.068	0.124	1	17.080	0.038	1	16.478	0.023	1
0000003	3.54563284	-74.56498337	18.550	0.042	99	17.536	0.015	99	16.710	0.009	99
0000004	3.55048180	-74.42867279	18.553	0.041	1	17.587	0.015	1	16.999	0.011	1
0000005	3.55086756	-74.34977722	18.149	0.133	1	17.314	0.044	1	16.670	0.028	1
0000006	3.55229902	-74.43345642	17.914	0.024	1	16.725	0.007	1	16.021	0.005	1
0000007	3.55510116	-74.50046539	18.416	0.036	1	17.444	0.014	1	16.870	0.010	1
0000008	3.55535913	-74.61768341	18.314	0.031	1	17.263	0.012	1	16.564	0.007	1
0000009	3.55825067	-74.28086853	18.147	0.028	1	17.534	0.015	1	17.135	0.012	1
0000010	3.56249487	-74.40327454	15.422	0.005	2	14.612	0.002	2	14.106	0.001	2
. . .	. . .	. . .	. . .	. . .	. . .	. . .	. . .	. . .	. . .	. . .	. . .

[1]Right Ascension: Degrees in the J2000 epoch.
[2]Declination: Degrees in the J2000 epoch.
[3]Flag: Number of stars used in determining magnitude. The '99' value represent that there are no stars satisfying our selection criteria (see Standardization subsection).

and *R*, respectively. Columns 5, 8, and 11 are their photometric errors, and columns 6, 9, and 12 are the number of frames that were used to derive the weighted mean magnitude. A star that did not satisfy our criteria as mentioned above was flagged as ‘99’ in these columns. The total number of survey stars is ~1.3 million across ~26 deg^2 of the SMC. The catalogue contains stars brighter than 19.0 magnitude in *B* (~0.73 million).

Completeness

Survey completeness: During the data reduction process, we found that a malfunction in the filter wheel system had caused the color filter to be misidentified. The result of this is an incomplete *BVR* data set, e.g., in the case of grid #07b there is no 60 s *B* filter exposure frame; this is actually a *V* filter image, thus giving a *VVR* data set. Such data sets were rejected from our catalogue. We also rejected non-photometric frames or chips caused by bad weather conditions. For these reasons, we estimated the survey completeness on the basis of the following definition: we assume a 100% survey completeness for a given grid if there are 60 s and 600 s exposure sets (i.e., *B*, *V*, and *R* in both) and if its dithered frame has a photometric condition for all chips. If better-dithered frames are available, we choose them in our calculation. On the basis of this survey completeness definition, we find an average of 95.1% survey completeness. Of course, it is higher than the actual completeness because one dithered frame cannot cover the gaps between each chip and some of the frames are not perfect photometric frames.

Photometric completeness: In order to estimate the accuracy of the photometry and to test the sampling completeness, the artificial star technique (Stetson and Harris, 1988; Stetson, 1991) was used in this study. Because our data sets have two exposure times for each filter frame, the limit of magnitude completeness depends on the 600 s frame in each field. Among the dithered frames for a given field, we performed the artificial star test for the first dithered frames suffixed as b, because they correspond to the mean area for grids having more than two ditherings. After fixing the number of artificial stars with respect to the instrumental magnitude ranges (see Stetson, 1991), we randomly generated positions and magnitudes using the random number function, ran2 (Press et al., 1992). We constrained the position to an area of [21:2024, 21:4074] to avoid placing stars near the edges on each chip. The results for two example grids are summarized in Table 2. Because stars brighter than 13 magnitude are saturated in our 600 s frames, we exclude stars above these magnitudes in our artificial star study. In general, the ~90% photometric completeness corresponds to a *B* magnitude of 18.5, although *B* is ~17.5 in crowded fields such as #06b-#11b and ~19.5 in sparse regions, for example, #20b, #21b, and #23b.

Comparisons with other catalogue

To check the accuracy of our data regarding astrometry and photometry, we compared our result with published catalogues. The catalogues used for the comparison with our data were the OGLE, MCPS, and Massey survey. The Optical Gravitational Lensing Experiment (OGLE, Udalski et al., 1998) group

Table 2. The results of the artificial star test for #07b and #28b fields. The values in each magnitude range are the average percentage for a mosaic (eight CCDs) image

		Magnitude ranges								
Field	Filter	13.5-14.5	14.5-15.5	15.5-16.5	16.5-17.5	17.5-18.5	18.5-19.5	19.5-20.5	20.5-21.5	21.5-
#07b	*B*	97.92	99.11	97.81	94.05	87.27	65.65	27.74	7.12	2.31
	V	97.92	97.99	94.74	87.41	68.69	38.31	10.82	3.66	2.40
	R	100.00	99.33	94.85	89.46	77.61	47.06	17.02	5.21	3.51
#28b	*B*	100.00	100.00	99.67	99.57	98.86	96.22	65.26	5.67	0.74
	V	100.00	100.00	99.45	99.58	98.24	95.69	53.28	3.34	0.46
	R	100.00	100.00	99.32	99.32	97.96	94.40	51.60	3.61	0.93

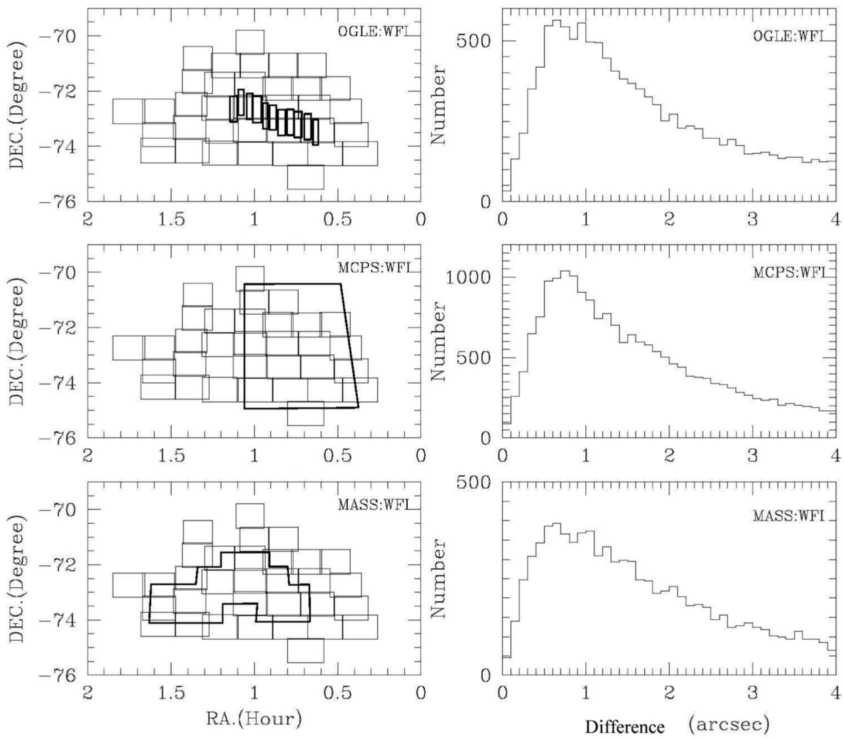

Fig. 4. Comparisons of survey areas and astrometric differences with other catalogues. The left panels are the comparison of grids and the right are the number distribution of astrometric solutions between our work and the comparison catalogues - OGLE, MCPS, and MASS. In the left panels the thin lines present our fields and the thick lines are others.

published *BVI* maps containing precise astrometric and photometric data for the central regions of the SMC bar. The estimated accuracy of their astrometry is 0.15 arcsec with a possible systematic error of up to 0.7 arcsec. The completeness of their data goes down to *B* ~20.0, *V* ~20.5, and *I* ~20.0 and the accuracy of the photometry is approximately 0.01 magnitude.

The Magellanic Clouds Photometry Survey (MCPS), performed by Zaritsky et al. (2002) contains a *UBVI* photometry and extinction map for the central 18 deg^2 area of the SMC. Considering the astrometric accuracy of MCPS, Zaritsky et al. (2002) compared their catalogue with that of Massey (2002) brighter than $V=15$ and found that the offset is less than 1" with the distribution peak at 0.3". Except in the dense region of the SMC, their photometric accuracy is at least *V* ~20.

Massey (2002) presented a *UBVR* CCD photometric survey for the 7.2 deg^2 of the SMC. In particular, because he was interested in brighter stars in the SMC, the photometric completeness of his catalogue is limited to *U*~*B*~*V* ~15.7 and *R* ~15.2. He used the Space Telescope Guide Star Catalog (GSC) to relate to celestrial coordinates. However, there is no mention of the astrometric accuracy of his catalogue stars.

Astrometry: The internal astrometric error in our survey data is estimated to be 0.5 arcsec because we fitted the astrometric solution using the MSCCMATCH task in the MSCRED package for each image within 0.5 arcsec, root mean square.

As a consistency check of our external errors, we compared our astrometry data (hereafter WFI) with the OGLE, MCPS, and Massey's survey (hereafter MASS). For the matching procedures, we used the Starlink program, TOPCAT, with maximum errors less than 7 arcsec in RA and DEC. The results are shown in Fig. 4 with survey field comparisons. In the figure,

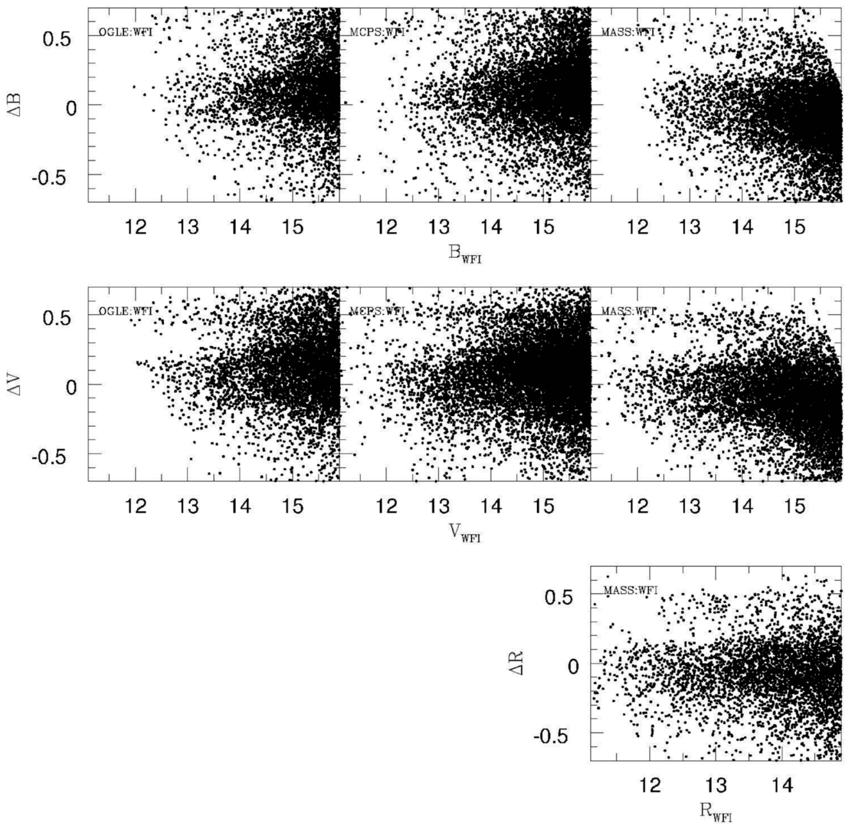

Fig. 5. Comparison of the photometric results with the OGLE, MCPS, and MASS catalogues for the brighter stars. The *x*-axis is our photometric magnitude and the *y*-axis illustrates the magnitude difference with respect to our data (WFI).

the left panel represents the comparison fields; the thin lines are our data and the thick lines are those of OGLE, MCPS, and MASS surveys, given at the top, middle, and bottom respectively. The right panel shows the number distribution of the astrometric solution difference between our data and the other catalogues. Although our survey extended to somewhat large radius ranges, the peak of the matching radius for all the comparison catalogues are within 1 arcsec. The peak radii are 0.6, 0.7, and 0.6 for OGLE, MCPS, and MASS data, respectively. It seems that there are no significant positional differences, although the external accuracy of astrometric solutions shows a tendency to extend about 2 arcsec in the distribution diagrams. These results are broadly in agreement with what one might expect given our plate scale, and the seeing during our observations.

Photometry: To test for photometric accuracy, we performed comparisons using the same stars used in astrometry solutions. We compared only *B* and *V* with OGLE and MCPS data because they have no *R* data, while *B*, *V*, and *R* can all be compared with MASS. The OGLE database has many stars (~2.2 million) despite its small survey area compared to the other catalogues. However, because the main aim of the OGLE project is to find gravitational lensing events, it gives more attention to faint stars. Thus, it contains fewer bright stars. In Fig. 5, we present the magnitude differences with respect to the three catalogues. The top, middle, and bottom panels are magnitude differences with respect to WFI in *B*, *V*, and *R*, respectively. Note that we only compared stars brighter than 16 magnitude in *BVR* with Massey (2002) because he was particularly interested in

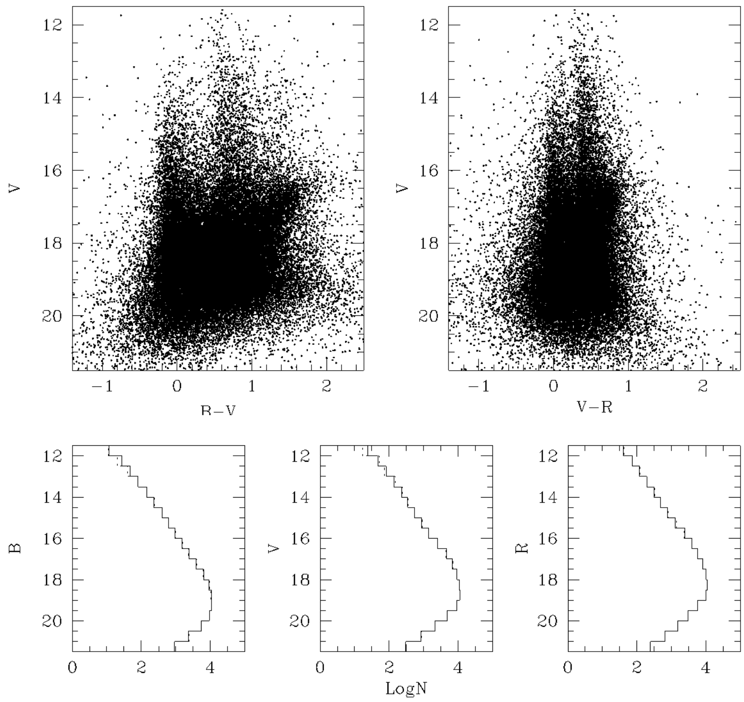

Fig. 6. The upper panels shows the *V* versus (*B–V*) and (*V–R*) CMDs of our SMC stars. Only about 5% of the sample is plotted to aid clarity. In the lower panel, the solid lines represent the number distribution for the stars used to construct the CMDs with the dashed lines for the total SMC stars. For the comparison, the dotted lines are normalized in 18 magnitude.

brighter stars. For the other catalogues, our data extended down to 17 magnitude in comparisons but cut off at 16 magnitude in the figure.

Although the differences show scattering up to 0.5 at 16 magnitude, the average magnitude differences are 0.077, 0.065, and −0.120 in *B*, and 0.105, 0.054, and −0.137 *V* in for the OGLE, MCPS, and MASS, respectively, while the ΔR between WFI and MASS is −0.164. A uniform difference of +0.5, covering the whole magnitude range, seems to be caused by the use of a larger matching limit in the astrometry solution. According to the average magnitude differences with respect to magnitude bins, however, our catalogue stars match well with MASS for stars brighter than 15 magnitude, and with OGLE for the ones fainter than 16 magnitude.

Color magnitude diagrams

With our *BVR* photometric data of the SMC, we constructed composite color magnitude diagrams for the whole SMC grid. However, for clarity, we have randomly selected 5% of the stars from the 1.3 million, and Fig. 6 shows *V* against (*B−V*) and *V* against (*V–R*), together with their number distributions.

As mentioned before, our photometric data are complete to around 18 magnitude, which can be confirmed from the number distribution diagrams; the peak values are around *B* ~19.0, *V* ~18.5, and *R* ~18.0. Considering stars brighter than 18 magnitude, we see three branches in *V* against (*B−V*); (*B−V*) ~0, between (*B−V*)=0.6 and 1.2, and a diagonal branch starting around *V*=16.5 and (*B−V*) ~1.8. These features are less clear in the *V* versus (*V−R*) plot. Stars located vertically along (*B−V*) ~0 are primarily unreddened massive main-sequence stars burning Hydrogen in their cores. To account for the broad clump (ranging from 0.6 to 1.2 in *B−V*), Massey (2002) argued that they are contaminated by foreground Galactic stars. He studied quantitatively the degree of domination using the Bahcall and Soneira (1980) model with the expected foreground contamination percentage shown in Fig. 7 of his paper. The third feature is the red giant branch and/or asymptotic giant branch, in which stars are burning helium.

Astronomical parameters: In this study, we discuss the color excesses, $E(B-V)$ and $E(V-R)$, interstellar extinctions, A_V and A_R, and distance modulus using the SMC spectroscopic data from the Evans et al. (2004) 2dF survey catalogue, which contains over 4000 stars. However, from 4161 2dF spectra, 323 stars have only spectral type without luminosity class, 79 show an ambiguous spectral type according to the authors, 2223 are only broadly classified, such as 'B0-5 (V)', and 22 are peculiar stars including two Wolf-Rayets. We removed those stars and used the remaining 1514 stars, which comprise 194 supergiants, 864 bright giants, 211 giants, 77 subgiants, and 169 dwarfs. For the photometry data, we used stars observed twice or more for the accuracy of magnitudes.

Color excess and extinction: There have been many studies on the relationship between intrinsic color and spectral type. Johnson (1966) presented intrinsic colors with respect to the MK system in many color indices for supergiants/giants and the main sequences. We derived $E(V-R)$ from relations for the main sequences and supergiants given in Johnson (1966), although the intrinsic colors are studied only for the late type in giants, from G5 to M6, contrary to most of 2dF and WFI stars, which are mostly O, B, and A types.

In evaluating $E(B-V)$, we adopted $(B-V)_0$ from Fitzgerald (1970) because it contains data for all luminosity classes, especially the bright giant stars that contribute the largest group in the 2dF catalogue. In order to estimate the intrinsic colors for each spectral type bin, we performed a high-order polynomial fit. In the Evans et al. (2004) catalogue, the latest spectral type is G8; therefore, we choose that as the lower limit to the fits. Since extrapolation sometimes shows spurious results, especially in high-order fitting, we restricted the spectroscopic data to lie between the upper and the lower limits in the luminosity class.

Table 3. The color excess values with respect to luminosity classes

Class	$E(B-V)$	$E(V-R)$
Supergiant (I)	0.062±0.147 (74)	0.040±0.130 (74)
Bright giant (II)	0.070±0.164 (378)	
Giant (III)	0.103±0.150 (91)	
Subgiant (IV)	0.156±0.137 (36)	
Dwarf (V)	0.131±0.120 (74)	0.090±0.084 (73)
Total	0.086±0.156 (653)	0.064±0.112 (147)

The resulting values with respect to the luminosity class are summarized in Table 3, together with the number of stars used in each class. The number of stars used in deriving $E(V-R)$ in dwarfs is one less than that for $E(B-V)$, because of the differences in the upper limits of the fits. As a cross-verification, we adopted the relations from Flower (1977) and Schmidt-Kaler (1982) in the calculation of $E(B-V)$ and found that there are no significant differences.

It is generally known that the SMC has a small and uniform foreground reddening of ~0.019 (e.g., McNamara and Feltz, 1980). Grieve and Madore (1986) studied the total reddening of the SMC with 46 supergiants from the Azzopardi and Vigneau (1975) and Feast et al. (1960) catalogue and formed $E(B-V)$ ranging from 0.09 up to 0.2. Massey et al. (1995) also found the same result using the reddening-free Q parameter with 179 SMC stars. More recently Larsen et al. (2000) reinforced this result from the study of B-type field stars and suggested a value of 0.07±0.02 in $E(B-V)$ color excess. The mean value of our $E(B-V)$ shows a good agreement with those studies.

After calculation of the color excesses, we derived the interstellar extinctions using the R_V=3.1 value (e.g., Schultz and Wiemer, 1975; Sneden et al., 1978). We plot the normalized number distribution for the $-0.3 \le A_V \le 0.9$ range in Fig. 7, in which the mean value of the interstellar extinction is ~0.225, taken between two peak values, corresponding to $E(B-V)$=0.076. This is also in reasonable agreement with our mean value of 0.086. However, it still shows a tail after the peak values.

In deriving A_R, we simply used the relation between A_V and $E(V-R)$, that is,

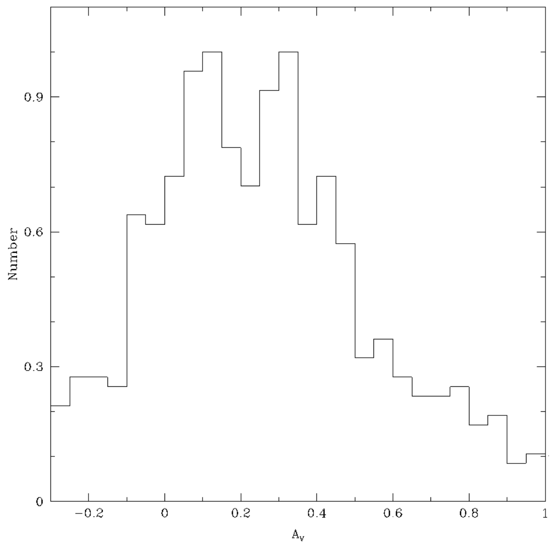

Fig. 7. The normalized number distribution of interstellar extinction values for the ranges of $-0.3 \leq A_V \leq 0.9$.

$$A_R = A_V - E(V-R) = 0.160, \qquad (2)$$

where $E(V-R)=0.065$. When we consider the uncertainties in the photometry, this value approximately matches the value of $A_R=0.194$ calculated from the Howarth (1983) formula:

$$A_R = 2.25E(B-V), \qquad (3)$$

where $E(B-V)=0.086$.

Distance modulus: Schmidt-Kaler (1982) gave a tabulation of the relationship between the spectral type and absolute magnitude (M) for each luminosity class. Conti et al. (1983) presented a more detailed relation of M_V to the spectral type for O-type supergiants, giants, and dwarfs. Humphreys and McElroy (1984) also compiled results for all luminosity classes, but it is limited to types later than B5, except for dwarfs. Therefore, we mainly adopt the Schmidt-Kaler (1982) values, supplemented with Conti et al. (1983) for the O stars. In the same way that we calculated the spectral type-intrinsic color relations, we performed high-order polynomial fits in order to interpolate between each spectral bin. In addition, we constrained the lower limit to G8. After calculating the absolute magnitudes, we find a mean distance modulus ($\overline{DM}$) of the SMC from the following equation with the derived mean A_V (i.e., $\overline{A_V}$) value:

$$\overline{DM} = \frac{1}{N}\sum_{i}^{N}(V-M_V)_i - \overline{A_V}, \text{ where } N=147. \qquad (4)$$

Adopting $E(B-V)=0.086$ (then $\overline{A_V}=0.267$), we get a mean distance modulus of 18.55±1.05. van den Bergh (2000) summarized the various methods of distance determination and suggested that the true distance modulus of the SMC is 18.85 (i.e., 58.9 kpc), with ~0.1 uncertainty. Recently, Harries et al. (2003) and Hilditch et al. (2005) studied the eclipsing binaries in SMC and obtained the distance modulus as 18.91± 0.10 (systematic), one the most precise determinations to date. Therefore, our determination is a little smaller than the published results, although it matches within our large uncertainty.

Summary

The SMC has received much attention because of its proximity and low metallicity. Hence, it is one of the most well studied astronomical objects. However, due to its large size in the sky, most studies have been concentrated on a part of the SMC, such as clusters or OB associations. In order to study macroscopic features of the SMC stars, we performed a *BVR* photometric survey with a WFI mosaic system mounted on a 40-inch telescope at the SSO during three epochs: September and October 2001 and November 2002. Mainly because of the weather conditions, the survey completeness is 95.1% for the planned 35 fields (~26 deg^2). In addition, on the basis of the artificial star technique, we found a 90% photometric completeness around 18.0 magnitude in *B*. The total obtained number of catalogue stars is ~1.3 million and the number brighter than 19 magnitude in *B* is ~0.73 million. From the estimate of the survey and photometric completeness, we believe that our SMC catalogue has 85.6% completeness up to 18.0 magnitude in *B*.

Using the 2dF spectroscopic data from Evans et al. (2004), we found the 0.086 and 0.065 color excesses in $(B-V)$ and $(V-R)$, which agree well with published results. From the derived $E(B-V)$ value, the extinction in V is 0.225 assuming R_V=3.1 and 0.160 in R. Finally, we also determined the distance modulus of the SMC, 18.55±1.05, a value that is slightly less than that of other results although it matches within uncertainty. On the basis of this study, we plan to publish results of the initial mass function and star formation histories of the SMC using population synthesis techniques.

Acknowledgment

This work was supported by research grants from the Catholic University of Daegu in 2013.

References

Arp, H., 1962, Stellar Content of Galaxies. In McVittie, G.C. (eds.), Problems of Extra- Galactic Research. IAU Symposium no. 15, Macmillan Press, New York City, NY, USA. 42-48.

Azzopardi, M. and Vigneau, J., 1975, List of 506 Stars, Probable Small Magellanic Cloud Members. Astronomy and Astrophysics Supplement, 22, 285-321.

Azzopardi, M. and Vigneau, J., 1982, Catalogue of the Small Magellanic Cloud Star Members. Astronomy and Astrophysics Supplement, 50, 291-376.

Bahcall, J.N. and Soneira, R.M., 1980, The Universe at Faint Magnitudes. I - Models for the Galaxy and the Predicted Star Counts. The Astrophysical Journal Supplement, 44, 73-110.

Bonanos, A.Z., Lennon, D.J., Köhlinger, F., van Loon, J.Th., Massa, D.L., Sewilo, M., Evans, C.J., Panagia, N., Babler, B.L., Block, M., Bracker, S., Engelbracht, C.W., Gordon, K.D., Hora, J.L., Indebetouw, R., Meade, M.R., Meixner, M., Misselt, K.A., Robitaille, T.P., Shiao, B., and Whitney, B.A., 2010, Spizer SAGE-SMC Infrared Photometry of Massive Stars in the Small Magellanic Cloud. The Astronomical Journal, 140, 416-429.

Conti, P.S., Garmany, C.D., de Loore, C., and Vanbevern, D., 1983, The Evolution of Massive Stars - The Numbers and Distribution of O Stars and Wolf-Rayet Stars. The Astrophysical Journal, 274, 302-312.

Evans, C.J., Howarth, I.D., Irwin, M.J., Burnley, A.W., and Harries, T.J., 2004, A 2dF Survey of the Small Magellanic Cloud. Monthly Notices of the Royal Astronomical Society, 353, 601-623.

Feast, M.W., Thackeray, A.D., and Wesselink, A.J., 1960, The Brightest Stars in the Magellanic Clouds. Monthly Notices of the Royal Astronomical Society, 121, 337-385.

Fitzgerald, M.P., 1970, The Intrinsic Colours of Stars and Two-Colour Reddening Lines. Astronomy and Astrophysics, 4, 234-243.

Flower, P.J., 1977, Transformations from Theoretical H-R Diagrams to C-M Diagrams. Astronomy and Astrophysics, 54, 31-39.

Grieve, G.R. and Madore, B.F., 1986, Photometric Studies of Magellanic Cloud Supergiants. I - Mean Magnitudes and Reddenings. II - Variability. The Astrophysical Journal Supplement, 62, 427-449.

Harries, T.J., Hilditch, R.W., and Howarth, I.D., 2003, Ten Eclipsing Binaries in the Small Magellanic Cloud: Fundamental Parameter and Cloud Distance. Monthly Notices of the Royal Astronomical Society, 339, 157-172.

Hilditch, R.W., Howarth, I.D., and Harries, T.J., 2005, Five Eclipsing Binaries in the Small Magellanic Cloud: Fundamental Parameter and Cloud Distance. Monthly Notices of the Royal Astronomical Society, 357, 304-324.

Howarth, I.D., 1983, LMC and Galactic Extinction. Monthly Notices of the Royal Astronomical Society, 203, 301-304.

Humphreys, R.M. and McElroy, D.B., 1984, The Initial Mass Function for Massive Stars in the Galaxy and the Magellanic Clouds. The Astrophysical Journal, 284, 565-577.

Johnson, H.L., 1966, Astronomical Measurements in the Infrared. Annual Review of Astronomy and Astrophysics, 4, 193-206.

Larsen, S.S., Clausen, J.V., and Storm, J., 2000, Reddenings and Metallicities in the LMC and SMC from Strömgren CCD Photometry. Astronomy and Astrophysics, 364, 455-466.

Lee, K.-W., 2005, A Photometric Survey of the Small Magellanic Cloud. Unpublished Ph.D. dissertation, University College London, London, UK, 225 p.

Lequeux, J., Peimbert, M., Rayo, J.F., Serrano, A., and Torres-Peimbert, S., 1979, Chemical Composition and Evolution of Irregular and Blue Compact Galaxies. Astronomy and Astrophysics, 80, 155-166.

Massey, P., 2002, A *UBVR* CCD Survey of the Magellanic Clouds. The Astrophysical Journal Supplement, 141, 81-122.

Massey, P., Johnson, K.E., and DeGioia-Eastwood, K., 1995, The Initial Mass Function and Massive Star

Evolution in the OB Associations of the Northern Milky Way. The Astrophysical Journal, 454, 151-171.

McNamara, D.H., Feltz, K.A.Jr., 1980, The Galactic Foreground Reddening in the Direction of the Magellanic Clouds. Publications of the Astronomical Society of the Pacific, 92, 587-591.

Mink, D.J., 1996, Browsing Images in World Coordinate Space with SAOimage. Astronomical Data Analysis Software and Systems, 101, 96-99.

Mink, D.J., 1997, WCSTools: Image World Coordinate System Utilities. Astronomical Data Analysis Software and Systems, 125, 249-252.

Mink, D.J., 1999, WCSTools: An Image Astrometry Toolkit. Astronomical Data Analysis Software Systems, 172, 498-501.

Press, W.H., Teukolsky, S.A., Vetterling, W.T., and Flannery, B.P., 1992, Numerical Recipes in Fortran. Cambridge University Press, Cambridge, UK, 933 p.

Schmidt-Kaler, Th., 1982, Stars and Star Clusters. In Schairfers, K. and Vogit, H.H., (eds.), Londolt-Börnstein: Numerical data and Functional Relationships in Science and Technology, Springer, Berlin, Germany, 1-34

Schultz, G.V. and Wiemer, W., 1975, Interstellar Reddening and IR-excess of O and B Stars. Astronomy and Astrophysics, 43, 133-139.

Sneden, C., Gehrz, R.D., Hackwell, J.A., York, D.G., and Snow, T.P., 1978, Infrared Colors and the Diffuse Interstellar Bands. The Astrophysical Journal, 223, 168-179.

Stetson, P.B., 1987, DAOPHOT: A Computer Programs for Crowded-Field Stellar Photometry. Publications of the Astronomical Society of the Pacific, 99, 191-222.

Stetson, P.B., 1991, On Deriving Globular-Cluster Luminosity Functions from CCD Observations, with a Particular Application to the Main-Sequence Turnoff/Subgiant Branch in Metal-Poor Clusters. In James, K.A. (eds.), The Formation and Evolution of Star Clusters, ASP Conference Series Vol. 13, Astronomical Society of Pacific, San Francisco, CA, USA, 88-111.

Stetson, P.B. and Harris, W.E., 1988, CCD Photometry of the Globular Cluster M92. The Astronomical Journal, 96, 909-1161.

Udalski, A., Szymański, M., Kubiak, M., Pietrzyński, G., Woźniak, P., and Źebruń, K., 1998, The Optical Gravitational Lensing Experiment Eclipsing Binary Stars in the Small Magellanic Cloud. Acta Astronomica, 48, 147-174.

Valdes, F.G., 2002, The Reduction of CCD Mosaic Data. In Gupta, R., Singh, H.P., and Bailer-Jones, C.A.L. (eds), Automated Data Analysis in Astronomy, Narosa Publishing, London, UK, 309 p.

van den Bergh, S., 2000, The Galaxies of the Local Group. Cambridge University Press, Cambridge, UK, 348 p.

Westerlund, B.E., 1997, The Magellanic Clouds. Cambridge University Press, Cambridge, UK, 292 p.

Zaritsky, D., Harris, J., Thompson, I.B., Grebel, E.K., and Massey, P., 2002, The Magellanic Clouds Photometric Survey: The Small Magellanic Cloud Stellar Catalog and Extinction Map. The Astronomical Journal, 123, 855-872

Manuscript received: July 12, 2013
Revised manuscript received: August 19, 2013
Manuscript accepted: September 12, 2013